

Original Research Article

Anti-inflammatory and anti-neuropathic effects of a novel quinic acid derivative from *Acanthus syriacus*

Karim M. Raafat

Department of Pharmaceutical Sciences, Faculty of Pharmacy, Beirut Arab University, 115020 Beirut, Lebanon

Article history:

Received: Aug27, 2018

Received in revised form:
Sep17, 2018

Accepted: Oct09, 2018

Vol. 9, No. 3, May-Jun 2019,
221-236.

*** Corresponding Author:**

Tel: 0096176014620

Fax: 00961 1300110

k.raafat@bau.edu.lb

Keywords:

Novel quinic acid derivative

Acanthus syriacus

Anti-inflammatory

Antinociceptive effects

Kromeic acid

Abstract

Objective: *Acanthus syriacus* (AS) is one of the valuable herbal plants with immunomodulatory potentials. The aim of this study is to assemble a phytochemical investigation of *A. syriacus* exploring its anti-inflammatory and antinociceptive properties, identification of its most active compound(s) and elucidating their structure and determining their mechanisms of action.

Materials and Methods: Bio-guided fractionation and isolation-schemes were used utilizing RP-HPLC, CC, ¹H- and ¹³C-NMR, and biological-models were used to evaluate their effects against inflammation and neuropathic-pain (NP).

Results: The outcomes showed that the most active fraction (FKCA) of AS was identified. Two of the three components of FKCA were identified by chromatographic-methods, while the third compound was isolated, its structure was elucidated and its was named Kromeic acid (KRA); FKCA contained Ferulic acid (27.5%), kromeic acid (48.1%), and chlorogenic acid (24.4%). AS, FKCA and KRA showed significant ($p < 0.05$) anti-inflammatory and antinociceptive potentials in the management of allodynia and thermal-hyperalgesia in NP. AS and FKCA showed comparatively equipotent antinociceptive-effects. FKCA showed higher antinociceptive effects than KRA suggesting additive-effects among FKCA components. The anti-inflammatory, insulin secretagogue, oxidative-stress reducing, and protective effects against NO-induced neuronal-toxicity might be amongst the possible mechanisms of tested compounds to alleviate NP.

Conclusion: Here, we report the isolation and structure elucidation of a novel quinic-acid derivative, KRA. *A. syriacus*, FKCA, and KRA might be used as a novel complementary approach to ameliorate a variety of painful-syndromes.

Please cite this paper as:

Raafat KM. Anti-inflammatory and anti-neuropathic effects of a novel quinic acid derivative from *Acanthus syriacus*. Avicenna J Phytomed, 2019; 9(3): 221-236.

Introduction

The *Acanthus* genus belonging to the Acanthaceae family which is a large plant family consisting of 250 genera and 2700 species distributed widely across the Mediterranean and tropical regions of the world (Capanlar et al., 2010). The majority of the *Acanthus* species have been used in Asian traditional medicine for amelioration of various ailments. Various *Acanthus* species have shown anti-hepatotoxic, antioxidant, antimicrobial, antitumor, antiviral, anti-inflammatory, analgesic, and anti-fertility activities (Asongalem et al., 2004; Babu et al., 2001,2002; Bravo et al., 2004; Capanlar et al., 2010). The major constituents of various *Acanthus* species were determined to be alkaloids, flavonoids, glycosides, saponins, and lignans (Bravo et al., 2004; Capanlar et al., 2010). In Lebanon, *Acanthus syriacus* is one of the endemic species that has been used as a folk medicine for its immunomodulatory properties and against various neurological disorders (Baydoun et al., 2015).

The carrageenan *in-vivo* experiments are widely accepted-models for assessment of the anti-inflammatory effects of compounds and are principally used for the evaluation of the acute-anti-inflammatory potentials of natural or synthetic compounds (Willoughby and DiRosa, 1972).

Neuropathic pain (NP) is amongst the most difficult pain types to treat after being provoked as a complication of many ailments including diabetes (Ziegler, 2008). High blood glucose level was shown to provoke allodynia and hyperalgesia in response to chemical or thermal nociceptive provocation (Pabbidi et al., 2008). The NP pathogenesis is multifactorial and the involved mechanisms are not fully understood (Taliyan and Sharma, 2012). Hyperglycemia also causes reactive-oxygen species (ROS) over-production and innate antioxidant defenses aggravation, increasing the oxidative stress which is an NP fundamental mechanism (Ozkul et al.,

2010). Hyperglycemia provoked oxidative stress and advanced glycation end-product generation leading to stimulation of pro-inflammatory cytokines (CKs) (Cameron and Cotter, 2008). Pro-inflammatory CKs provoke nitric oxide (NO) synthase expression and elevate NO production (Yu et al., 2009; Taliyan and Sharma, 2012). Moreover, NO is involved in allodynia and hyperalgesia causing the NP (Joharchi and Jorjani, 2007; Taliyan and Sharma, 2012).

Currently, different classes of non-steroidal anti-inflammatory drugs, opioids, antidepressants, and anticonvulsants are used for amelioration of NP; nevertheless, the limited pain relief is achieved due to their partial-efficiency and recorded toxicities (Ziegler, 2010). Thus, there is an increasing need to discover more efficient and safer drugs for the management of NP. Alternative medicines have gained a reputation in the management of NP, and many indigenous medicinal plants were found to be effective in ameliorating NP (Comelli et al., 2009; Raafat et al., 2017b; Raafat and Hdaib, 2017; Taliyan and Sharma, 2012). Moreover, there is an increasing necessity for deeper investigation of these complementary medicines to understand their chemical compositions and identify their potential compounds and their mechanisms of actions to be used for NP amelioration.

A. syriacus is a promising herbal remedy. However, to date, there are no deep phytochemical or biological reports about *A. syriacus*.

Therefore, the aim of the present study is to assemble a phytochemical investigation of *A. syriacus* exploring its anti-inflammatory and antinociceptive properties, identification of its most active compound(s), elucidating active compounds structure and discovering their possible mechanisms of action.

Materials and Methods

Standards and solvents were commercially obtained from Merck-Sigma-Aldrich (Germany).

Plant material

The aerial parts of *A. syriacus* were collected from Yahchouch, Kesrwan, Mount Lebanon (N 34° 04' 09" E 35° 44' 20", Lat: 34.0692911 Lng: 35.7387591), during the flowering stage in the middle of May 2016. The specimen was authenticated with a reference sample and a specimen was deposited in the faculty herbarium with the voucher (No. FP-16-41).

Extraction

The aerial parts of *A. syriacus* were dried in shade and size-reduced by G. Ming Mill (China) to form a powder. The dried powder was defatted by hexane and then, sonicated twice using 80% ethanol for 6hr at room temperature. Then, the extract was dried under vacuum at 40°C by Buchi rotary-evaporator (Germany) and then lyophilized utilizing Edwards freeze drier (Germany). The extract was kept frozen at -40°C until further utilization.

HPLC-PDA analysis: *A. syriacus* whole extract standardization

The *A. syriacus* whole ethanolic extract was analyzed utilizing MultoHigh 100 RP18-5 μ (Germany) as a reversed phase-high performance liquid chromatography (RP-HPLC) column at 40 °C. The developer was comprised of gradient-elution of (A) Milli-Q distilled water (formic acid 0.1%) and (B) methanol: 0min 90%A; 5 min 72%A; 9 min 55%A; and 14 min 20%A; 5 μ L injection-volume, and flow rate was 1mL/min. The detection wavelength range was 200–600nm focusing on 254nm.

A. syriacus Bio-guided fractionation and isolation

The extract was then fractionated utilizing silica gel column-chromatography (75 \times 15 cm). The column was developed by a gradient mobile phase: one bed volume

(BV) of hexane/ethyl acetate (50:50, v/v), then one BV EtAc, then one-BV of EtAc/water/formic acid (46:46:8, v/v), then 2 BV of EtAc, formic acid, water and hexane (70:7.5:7.5:15, v/v/v/v), then 1 BV ethanol/water (50:50, v/v), and finally one BV 100% water. Fractions were collected every 2 min. and similar fractions were combined and concentrated under reduced pressure. In order to identify the most active compound (s), each fraction was evaluated in the same-way as the *A. syriacus* extract for its antinociceptive properties. Most fractions were identified by steeping method utilizing the RP-HPLC system and utilizing reference standards. Peak nine was (Figure 1) identified utilizing ¹H and ¹³C NMR analysis.

Sample preparation for ¹H and ¹³C NMR investigation

The NMR experiments were done using a Bruker 300 MHz spectrometer (Germany) equipped with an auto-sampler. NMR samples were prepared by dissolving the isolated compound(s) in deuterated methanol (MeOH-d₄, Sigma-Aldrich). NMR spectra ¹³C-HSQC (Hetero-nuclear single quantum coherence), ¹³C-HMBC (Hetero-nuclear Multiple Bond coherence), ROESY NMR (Rotating-frame Overhauser Effect Spectroscopy) and COSY NMR (Correlation Spectroscopy) were obtained at 300 MHz, at 25°C.

Animals

Male albino mice (22-30g) were accommodated for one week prior to the *in vivo* experiment. The animals had free-access to water and standard feeding pellets (except otherwise stated), and were kept under 12hr/12hr dark/light cycles. All experiments were done according to animal-care rules and regulations, and approved by BAU Institutional Review Board (2019A-0056-P-R-0297).

Acute carrageenan-provoked inflammatory-pain

In order to assess the acute carrageenan-induced inflammatory-pain, 100 μ L of 1% carrageenan-solution was intraplantarly injected into the mice left hind-paw (n=7/group). The positive control (ibuprofen 100mg/kg) was orally-administered 0.5hr prior to carrageenan injection as described previously (Gardmark et al., 1998; Salama et al., 2016). The vehicle control (VEH) animals were injected intraplantarly with 100 μ L vehicle only (saline). Then, 120 min post-carrageen-injection, behavioral-measurements were performed.

Diabetes induction

Diabetes was induced in mice by injecting 180mg/kg alloxan every other day for three days. The blood glucose level (BGL) was checked by pricking the animal tail and utilizing Accu-chek glucometers (Germany) (Jamalan et al., 2015; Khaneshi et al., 2013). The blood glucose levels (BGL) were measured acutely at hour 6 and subchronically for 8 days, and for 8 weeks. Sigma glucometers (Germany) were utilized to monitor BGL. The glycated-hemoglobin (HbA1c) level was monitored utilizing Analyticon HbA1c kits (Germany) for 8 weeks. Animals having BGL \geq 200 mg/dL and HbA1c > 8 were considered diabetic.

Experimental protocol

After confirmation of diabetes mellitus (DM) and NP after monitoring of basal nociceptive-reaction 8 weeks post-alloxan injection, mice were randomized to different groups (n=7/group), and scheduled to pre- and 8-week post-treatment monitoring, as follows:

- Test groups: The *A. syriacus* ethanol extract (AS) (50, 100, and 150mg/kg), FKCA isolated fraction (FKCA) (5, 10, and 20mg/kg), kromeic acid (KRA) (5, 10, and 20mg/kg) were given to alloxan-induced diabetic-mice, and treated every other day for 8 weeks, and monitored pre- and 8-week post-treatment.

- Positive controls: The following positive standards were used: ibuprofen 100mg/kg (Ib) in inflammatory pain analysis, glibenclamide (5mg/kg) (GB) in HbA1c and serum insulin experiments, tramadol 10 mg/kg (TRA) in diabetic neuropathy experiments, and metformin 25mg/kg (MTF) in the biochemical studies.

- Vehicle control (VEH or DIA+VEH): Group of alloxan-induced vehicle-treated diabetic control mice.

- Normal control (NORM): Group of normoglycemic non-treated normal mice.

HbA1c and serum insulin levels

The glycated-hemoglobin (HbA1c) level was carefully monitored prior to treatment and eight-week post-treatment utilizing Analyticon HbA1c analytical columns. Moreover, the serum-insulin levels were measured pre- and 8-week post-oral administration using a reversed phase HPLC method utilizing RP-C18 endcapped Lichrospher-column (Merck) at 40°C with a flow-rate of 1ml/min. The solvent for HPLC was composed of trifluoroacetic acid (0.1%) in double-distilled water (DDW) (A) and acetonitrile (ACN) (B). The gradient-elution-conditions at 214 nm were as follows: 0 min 70% (A), and then 5min 60% (A), as described before (Raafat et al., 2017a; Raafat and Wael, 2018).

Oxidative-stress analysis

In order to evaluate the oxidative-stress, serum-catalase (CAT, kU/I) and reduced glutathione (GSH, μ g/mg) were monitored pre- and eight-week post-oral administration (Ellman, 1959; Yasmineh et al., 1995). Utilizing a modified method, the lipid peroxidation (LPO) levels have been evaluated by thiobarbituric acid(TBA) experiment (Ohkawa et al., 1979). Concisely, pre- and 8-week after-treatment, TBA (0.8%) was added to serum (0.2mL), sodium lauryl sulfate (SLS, 8.1%), and dilute HAc in DDW (20%). Following 60 min of heating at 95°C and then cooling-down, the combination was extracted using methanol/isopropyl alcohol (1:15, v/v), and

then the absorbance was measured by a JASCO-spectrophotometer (Japan) at 532 nm (Ohkawa et al., 1979).

Nociceptive responses assessment

Eight weeks after diabetes induction, animals were evaluated for diabetic-neuropathy success-rate (DNSR, significant losing sensory response to thermal-nociception below 10 sec (Sullivan et al., 2007). The DNSR was about 88% and the test compounds antinociceptive potentials were evaluated every other week for eight weeks.

Thermal-nociceptive latency evaluation

Animals with DNSR were involved in the thermal-hyperalgesia tail-flick and hot-plate latency experimentations (Micov et al., 2015). In brief, the animals were tested utilizing a hot-plate analgesia-meter (Ugo-Basile-Italy), or a tail-flick apparatus (Hugo-Sachs-Elektronik-Germany). The thermal-intensity was tuned to provide a baseline latency-time for the hot-plate test of 4–5 sec, and 1.5-2.5 sec for the tail-flick test for normal non-diabetic mice (NORM). A 10-sec cut-off time was adopted in thermal-nociceptive latency experiments to avoid tissue-damage.

Mechanical-nociceptive latencies evaluation

The tactile-allodynia, in mice with DNSR, was evaluated by monitoring the paw-withdrawal-thresholds (PWT) using Von-Frey-filaments (OptiHair) (Ohsawa et al., 2011). In brief, mice were separately put on a mesh floor in a bottom-up plastic cage. The force on the plantar-surface of the animal left hind-paw was gradually increased till it withdrew the paw. Here, 32 g cut-off force was adopted in the mechanical-nociceptive experiments for animal safety.

Nitric oxide (NO) levels measurement

NO level was determined by utilizing the Griess-reagent technique (Green et al.,

1982). Both urinary ($\mu\text{M/L}$) and tissue ($\mu\text{M/mg}$ protein) nitrite were measured.

Statistical analysis

Outcomes (mean \pm SEM) were statistically assessed by one way ANOVA followed up by the Student–Newman–Keuls analysis utilizing OriginPro® statistics-software. P -value <0.05 was regarded as statistically-significant.

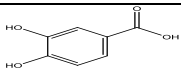
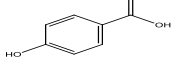
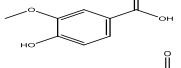
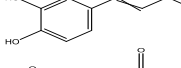
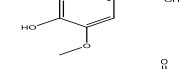
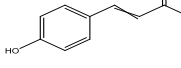
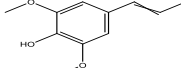
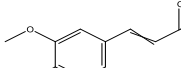
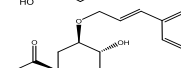
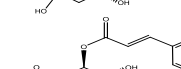
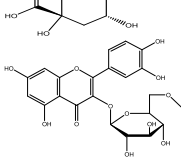
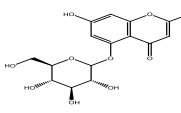
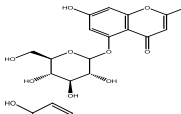
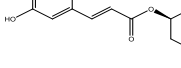
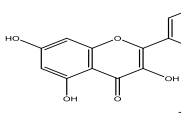
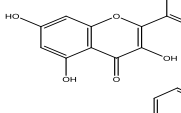
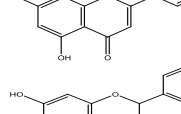
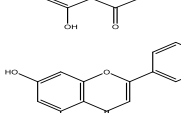

Results

HPLC-PDA analysis: *A. syriacus* whole extract standardization

HPLC-PDA analysis revealed the phenolic compounds present in the in *A. syriacus* ethanolic extract (Figure 1).The HPLC chromatogram showed 19 major peaks, from them 18 peaks were identified by steeping method utilizing standard curves. One compound (peak 9) was elucidated by ^1H and ^{13}C NMR as a novel quinic acid derivative and was named kromeic acid (Figure 1).The chemical structures and the percentages variation of the main compounds is presented in Table 1. The RP-HPLC major peaks were: (1) protocatechuic acid (3.47%), (2) p-hydroxybenzoic acid(6.47%), (3) vanillic acid (5.50%), (4) caffeic acid (3.60%), (5) syringic acid (3.12%), (6) p-coumaric acid (2.90%), (7) sinapic acid (3.41%), (8) ferulic acid (3.49%), (9) kromeic acid (6.10%), (10) chlorogenic acid (3.10%), (11) rutin (2.84%), (12) luteolin-glucoside (4.10%), (13) apigenin-glucoside (6.23%), (14) rosmarinic acid (8.43%), (15) quercetin (4.20%), (16) kaempferol(6.80%), (17) luteolin (3.80%), (18) naringenin (11.30%), and (19) apigenin (9.33%) (Figure1 and Table1). Quantitative tests showed that naringenin and apigenin were the most abundant phenolic compounds in the *A. Syriacus* ethanolic extract. Comparatively lower amounts of rutin, p-coumaric acid, and chlorogenic acid also remarkably distinguished *A. syriacus* sample (Figure 1).

Raafat

Table1. Phenolic components found in the RP-HPLC studied *A. syriacus* ethanolic extract.

Peak #	Compound	t _R (min)	Chemical structure	%
1	Protocatechuic acid	1.9		3.47
2	p-Hydroxybenzoic acid	2.2		6.47
3	Vanillic acid	2.4		5.50
4	Caffeic acid	2.5		3.60
5	Syringic acid	2.8		3.12
6	p-coumaric acid	3.2		2.90
7	Sinapic acid	4.0		3.41
8	Ferulic acid	4.4		3.49
9	Kromeic acid	4.8		6.10
10	Chlorogenic acid	5.4		3.10
11	Rutin	5.7		2.84
12	Luteolin-glucoside	6.9		4.10
13	Apigenin-glucoside	7.2		6.23
14	Rosmarinic acid	8.7		8.43
15	Quercetin	10.3		4.20
16	Kaempferol	11.4		6.80
17	Luteolin	13.7		3.80
18	Naringenin	15.1		11.30
19	Apigenin	17.4		9.33

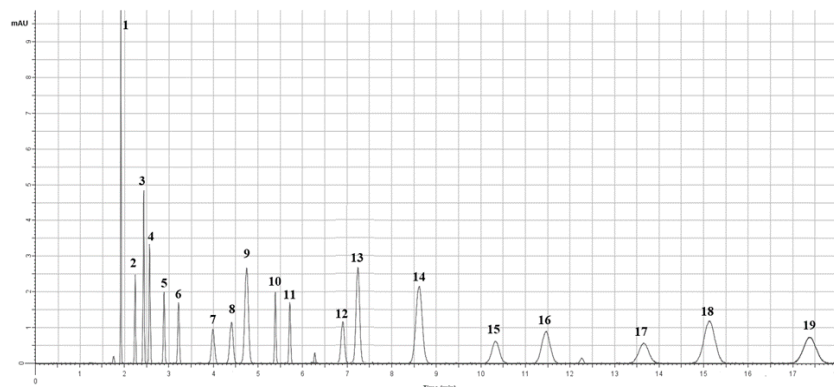


Figure 1. HPLC analysis of *Acanthus syriacus* EtOH extract: (1) protocatechuic acid, (2) p-hydroxybenzoic acid, (3) vanillic acid, (4) caffeic acid, (5) syringic acid, (6) p-coumaric acid, (7) sinapic acid, (8) Ferulic acid, (9) kromeic acid, (10) chlorogenic acid, (11) rutin, (12) luteolin-glucoside, (13) apigenin-glucoside, (14) rosmarinic acid, (15) quercetin, (16) kaempferol, (17) luteolin, (18) naringenin, and (19) apigenin.

A. syriacus bio-guided isolation, RP-HPLC, ¹H and ¹³C NMR structure elucidation and identification of the most active compounds

The most active fraction having antinociceptive potentials was isolated utilizing column-chromatography separation method. The RP-HPLC analysis, similar to the whole extract, was done for the most active fraction. Three compounds were recognized in this active fraction. Two compounds of the most active fraction were identified as ferulic acid and chlorogenic acid by steeping method utilizing reference standards. The third compound was isolated from the mixture by subjecting it to second silica-gel column-chromatography and was developed using dichloromethane and mixtures of dichloromethane and methanol with increasing polarities. Similar fractions were combined and concentrated. The third compound was further purified by semi-preparative HPLC. Compound 3 was obtained as an amorphous yellowish solid and identified by m/z: 340.1200 using Nano-ESI-MS in the positive mode, elemental analysis: C, 56.5%; H; 5.9%; O, 37.6%, and chemical formula C₁₆H₂₀O₈. The ¹H Spectral data (Table 2 and Figure 2) exhibited 2.14, dd (J=14.50, 2.79 Hz), 2.13, dd (J=14.50, 2.79 Hz), 2.34, dd (J=14.25, 2.79 Hz), 2.33, dd (J=14.25, 2.79 Hz), 3.18, t (J=2.79 Hz), 3.3, dt (J=10.26, 2.79 Hz), 3.40, q (J=2.79 Hz), 3.81, d (J=7.30 Hz),

3.81, d (J=7.30 Hz), 5.60, s, 5.90, s, 6.25, dt (J=17.56, 7.30 Hz), 6.50, d (J=17.56 Hz), 7.06, dd (J=8.56, 1.90 Hz), 7.41, dd (J=8.56, 1.90 Hz), 7.42, dd (J=8.60, 1.90 Hz), 9.48, s, 9.48, s. The three dd [7.06, dd (J=8.56, 1.90 Hz), 7.41, dd (J=8.56, 1.90 Hz), 7.42, dd (J=8.60, 1.90 Hz)] belonged to the aromatic protons. The olefinic protons were observed at 6.25, dt (J=17.56, 7.30 Hz), and 6.50 d (J=17.56 Hz). The quinic acid protons appeared at 2.14, dd (J=14.50, 2.79 Hz), 2.13, dd (J=14.50, 2.79 Hz), 2.34, dd (J=14.25, 2.79 Hz), 2.33, dd (J=14.25, 2.79 Hz), 3.18, t (J=2.79 Hz), 3.3, dt (J=10.26, 2.79 Hz), 3.40, q (J=2.79 Hz). The methylene group protons appeared as two duplets at δ 3.81. The main proton-proton neighboring interactions of the aromatic ring were detected between H-29 and H-30 in the COSY spectrum. The ¹³C NMR chemical shifts (Table 2) at δ114.8, δ 116.1, δ 123.0, δ 130.7, δ 132.3, δ 146.5, and δ 146.5 were assigned to the aromatic carbons. Comparison of the ¹³C NMR with HMQC and DEPT spectra revealed C₁₃ methylene group. The olefinic group carbon appeared at δ123.1 and δ132.3. The quinic acid carbons appeared at δ38.1, δ38.3, δ70.3, δ71.8, δ73.5, and δ74.5, with the carboxylic acid carbon observed at δ 180.4. The C₁₃ signal of the methylene group at δ66.6 exhibited a clear correlation with the olefinic proton at δ 123.1 in the HMQC spectrum. The HMBC spectrum of

the compound expounded a signal between the C₂ of the quinic acid and the H₃ of the methylene group (Table 2 and Figure 2). Therefore, the quinic acid derivative (compound 3) was named kromeic acid (KRA), and the most active fraction in *A. syriacus* (AS) was named FKCA due to its content of ferulic acid (27.5%), kromeic acid (48.1%), and chlorogenic acid (24.4%).

Table 2. Kromeic acid (KRA) ¹H -NMR and ¹³C-NMR data.

Position*	δ C	Position*	δ H, m, (J in Hz)
1	123.0	22	5.90, s
2	74.5	23	9.48, s
3	73.5	24	9.48, s
4	70.3	25	2.33, dd (J=14.25, 2.79Hz)
5	38.1	26	2.34, dd (J=14.25, 2.79Hz)
6	71.8	27	3.3, dt (J=10.26, 2.79Hz)
7	38.3	28	3.18, t (J=2.79Hz)
8	180.4	29	7.42, dd (J=8.60, 1.90Hz)
9	—	30	7.41, dd (J=8.56, 1.90Hz)
10	—	31	7.06, dd (J=8.56, 1.90 Hz)
11	—	32	6.50, d (J=17.56Hz)
12	—	33	6.25, dt (J=17.56, 7.30Hz)
13	66.6	34	3.81, d (J=7.30Hz)
14	—	35	3.81, d (J=7.30Hz)
15	123.1	36	2.13, dd (J=14.50, 2.79Hz)
16	132.3	37	2.14, dd (J=14.50, 2.79Hz)
17	116.1	38	3.40, q (J=2.79Hz)
18	146.5	39	5.60, s
19	146.5		
20	114.8		
21	130.7		

*As shown in Figure2.

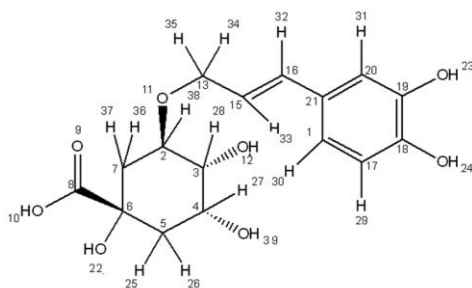


Figure 2. Kromeic acid (KRA) chemical structure

AS, FKCA and KRA potentials against inflammatory-pain

To evaluate AS, FKCA, and KRA anti-inflammatory activities, inflammation acute-phase was induced in a mouse model of paw-edema by carrageenan. Two hours after intraplantar carrageenan injecting to the animals, a significant ($p < 0.05$) mechanical hypersensitivity was induced ($n = 7/\text{group}$) (Figure 3). The PWT was

reduced from $8.84 \pm 0.19\text{g}$ in normal-mice (Normal) to $3.84 \pm 0.06\text{g}$ in the vehicle-control group (VEH). AS in a dose-dependent manner significantly ameliorated the carrageenan-induced edema ($n = 7/\text{group}$). As compared to VEH, AS (50, 100 and 150mg/kg) elevated PWT (i.e. reversed the mechanical-hypersensitivity) with 0.79, 1.16 and 1.23 folds, respectively. In a dose-dependent manner, the most active fraction (i.e. FKCA) and the isolated KRA significantly ameliorated the carrageenan-induced edema ($n = 7/\text{group}$). Compared to VEH, FKCA (5, 10 and 20mg/kg) elevated PWT by 1.00, 1.26 and 1.31 folds, respectively, whereas KRA (5, 10 and 20mg/kg) elevated PWT by 0.40, 0.45 and 0.82 folds, respectively (Figure 3). The efficiency of AS, FKCA, and KRA on reversing mechanical-hypersensitivity, proposes their capabilities to ameliorate acute inflammatory-pain.

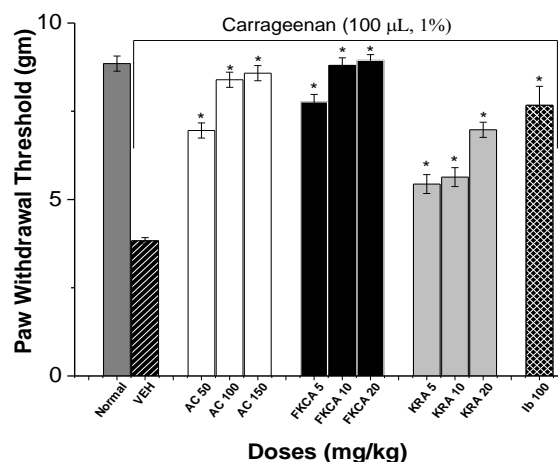


Figure 3. Inflammatory pain analysis. Carrageenan (100 μ L, 1%) was injected intraplantarly 2hr prior to the pain threshold assessment by the paw pressure test. Oral administration (gavages) of *Acanthus syriacus* (AC), FKCA isolated fraction (FKCA), and kromeic acid (KRA) 0.5hr before the test. Oral Ibuprofen 100mg/kg (Ib 100) was used as positive-control. "Normal" designates normal-mice. "*" means $p < 0.05$ compared to vehicle-control (VEH) ($n = 7/\text{group}$).

AS, FKCA and KRA potentials against BGL, HbA1c, and serum insulin

In the acute experiments, AS (50, 100 and 150mg/kg) reduced BGL by 45.4, 52.7 and 54.5%, 6hr post-administration,

Acanthus syriacus phytochemical and biological investigation

respectively, as compared to vehicle-treated diabetic control mice (DIA+VEH) (Figure 4A). When compared to DIA+VEH group, FKCA (5, 10 and 20mg/kg) reduced BGL by 49.1, 54.4 and 57.6%, 6hr post-administration, respectively (Figure 4B). KRA (5, 10 and 20mg/kg) decreased BGL by 40.6, 44.1 and 50.9%, 6hr post-administration, respectively. However, glibenclamide 5mg/kg (GB), produced 35.9% reduction in BGL (Figure 4C).

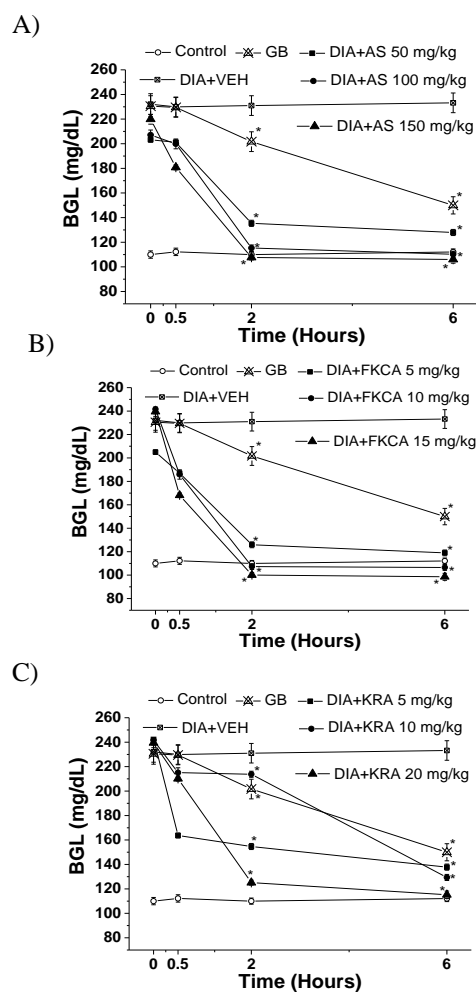


Figure 4. The acute effect of (A) *Acanthus syriacus* (AC), (B) FKCA isolated fraction (FKCA), and (C) kromeic acid (KRA) on blood glucose levels, utilizing glibenclamide 5mg/kg (GB) as positive control. "Control" designates normal non-diabetic mice. "*" designates significant differences at $p < 0.05$ when compared to vehicle-treated diabetic control (DIA+VEH) (n=7/group).

Moreover, subchronically, AS (50, 100 and 150 mg/kg) declined BGL by 37.9, 41.1 and 44.2%, 8-day post-administration, respectively, when compared to DIA control (Figure 5A). Compared to

DIA+VEH, FKCA (5, 10 and 20 mg/kg) declined BGL by 36.7, 37.7 and 51.1%, 8-day post-administration, respectively (Figure 5B); nevertheless, KRA (5, 10 and 20mg/kg) reduced BGL by 22.9, 33.1 and 43.9%, 8-day post-administration, respectively. GB caused a 30.5% reduction in BGL (Figure 5C).

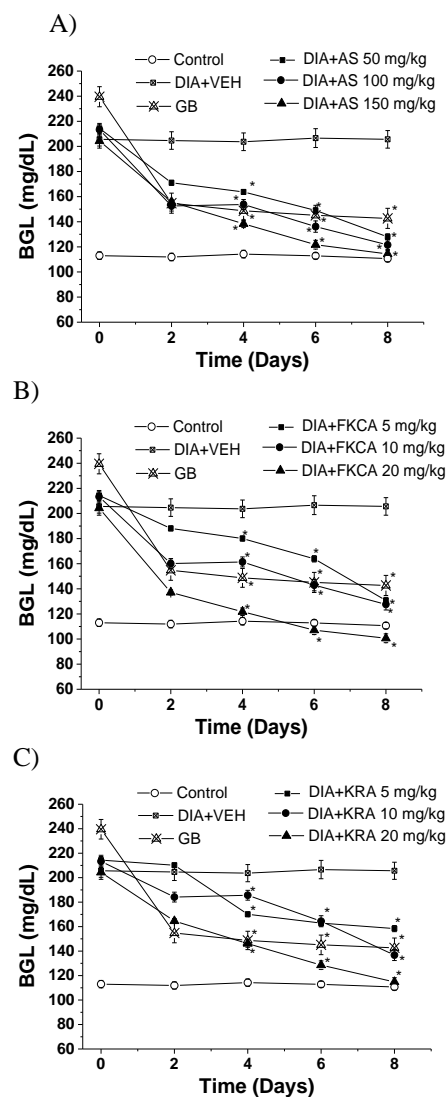


Figure 5. The subchronic effect of (A) *Acanthus syriacus* (AC), (B) FKCA isolated fraction (FKCA), and (C) kromeic acid (KRA) on blood glucose levels, utilizing glibenclamide 5mg/kg (GB) as the positive control. "Control" designates normal non-diabetic mice. "*" designates significant differences at $p < 0.05$ when compared to vehicle-treated diabetic control (DIA+VEH) (n=7/group).

Increasing doses of AS, FKCA, and KRA significantly and dose-dependently decreased HbA1c level 8-week post-administration (Figure 6). Compared to

VEH, AS (50, 100 and 150mg/kg) significantly reduced HbA1c by 10.8, 13.8 and 16.2%, respectively (Figure6). FKCA (5, 10 and 20mg/kg) also reduced the HbA1c levels 8-week post-administration by 9.9, 10.2 and 16.6%, respectively. KRA (5, 10 and 20mg/kg) ameliorated HbA1c by 8.1, 10.1 and 11.5%, respectively. However, GB caused a 8.4% reduction in the level of HbA1c (Figure 6).

To better evaluate AS, FKCA, and KRA antidiabetic mechanism, serum insulin levels were monitored. In a dose-dependent manner and after 8-weekoral administrations, AS, FKCA, and KRA significantly raised serum insulin level

(SIL) (Figure 7). AS (50, 100 and 150mg/kg) significantly raised SIL by 3.4, 3.8 and 4.4 folds, respectively, compared to VEH (Figure 7). As compared to VEH, FKCA (5, 10 and 20mg/kg) raised the SIL by 3.1, 3.4 and 4.9 folds, respectively, likewise, KRA (5, 10 and 20mg/kg) raised the SIL by 1.8, 2.1 and 2.8 folds, 8-week post-administration, respectively. In contrast, GB did not raise SIL significantly (Figure 7).

The potencies of AS, FKCA, and KRA on ameliorating BGL and controlling HbA1c levels, propose their potentials to control diabetes and NP.

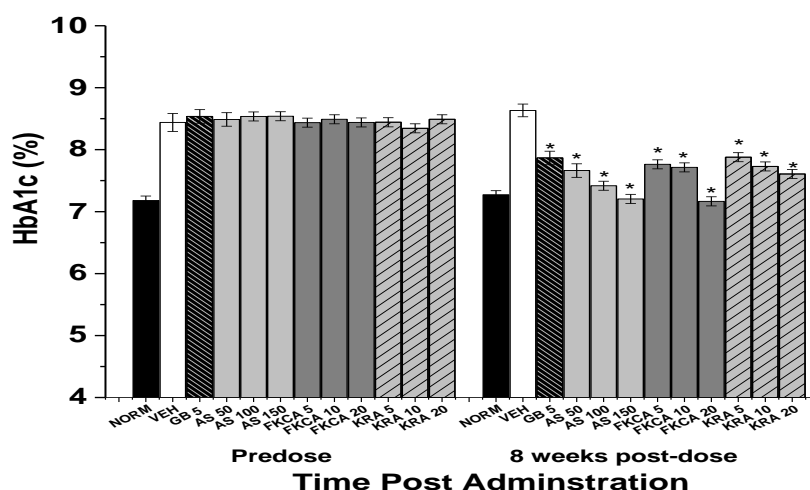


Figure 6. The effect of *Acanthus syriacus* (AC), FKCA isolated fraction (FKCA), and kromeic acid (KRA) (mg/kg) on HbA1c levels before (pre-dose) and 8 weeks after administration (8-week post-dose), utilizing glibenclamide 5mg/kg (GB) as positive control. “NORM” designates normal non-diabetic mice. “*” designates significant differences (p<0.05) as compared to vehicle-treated diabetic control (VEH), (n=7/group).

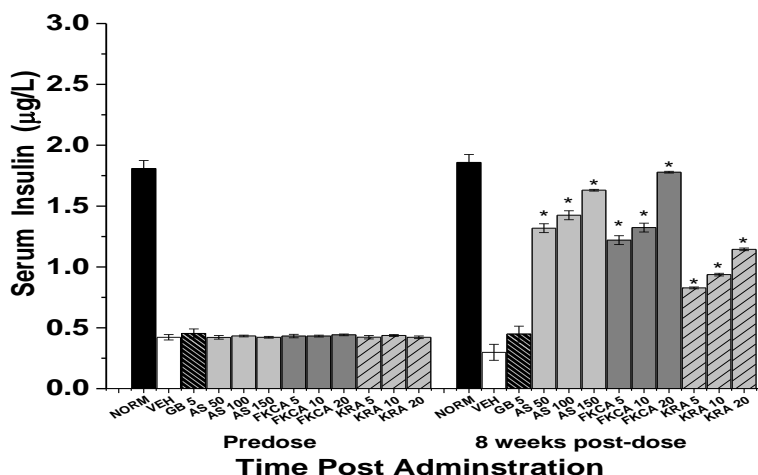


Figure7. The effect of *Acanthus syriacus* (AC), FKCA isolated fraction (FKCA), and kromeic acid (KRA) (mg/kg) on serum insulin levels before (predose) and 8 weeks after administration (8-week post-dose), utilizing glibenclamide 5mg/kg (GB). “NORM” designates normal non-diabetic mice. “*” designates significant differences (p<0.05) as compared to vehicle-treated diabetic control (VEH), (n=7/group).

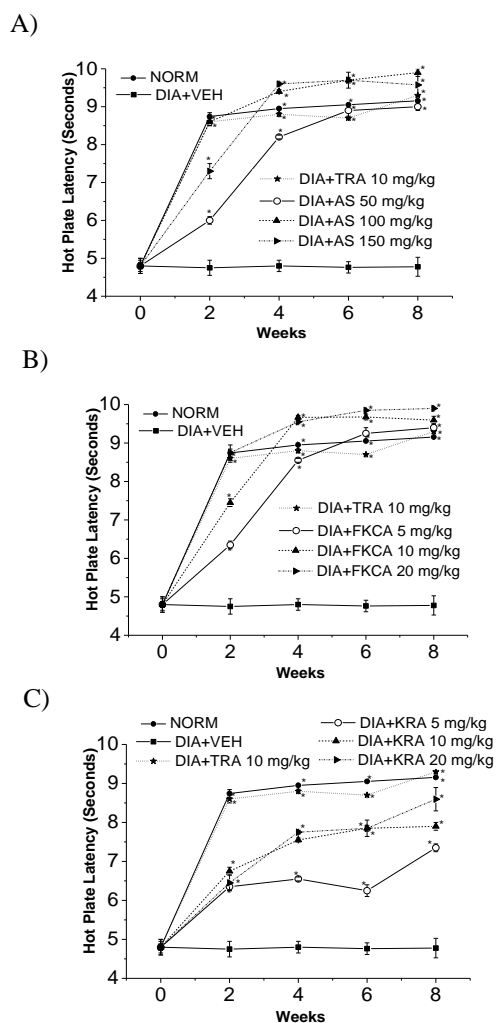


Figure 8. The effect of (A) *Acanthus syriacus*(AC),(B) FKCA isolated fraction (FKCA), and (C) kromelic acid (KRA) against hyperalgesia on the hot-plate latency in alloxan-treated mice with tramadol (TRA 10mg/kg) as a positive control. "NORM" designates normal non-diabetic mice. "*" shows significant differences at $p < 0.05$, compared to vehicle diabetic-control (DIA+VEH) (n=7).

Serum catalase (CAT), reduced glutathione (GSH), and lipid peroxide (LPO) levels

CAT, GSH, and LPO levels were measured at pre- and 8-week post-treatments, and compared to VEH. AS (50, 100 and 150mg/kg) significantly elevated CAT level by 1.32, 1.50, and 1.57 folds, increased GSH level by 87.5, 88.7, and 95.3%, and reduced LPO level by 92.3, 92.1 and 92.6%, respectively (Table 3). FKCA (5, 10 and 20 mg/kg) raised the CAT level by 1.28, 1.45 and 1.58 folds, increased GSH level by 84.8, 86.3, and 98.2%, and reduced LPO level by 92.1, 91.7 and

92.8%, respectively, KRA (5, 10 and 20mg/kg) raised the CAT level by 0.80, 0.94, and 1.01 folds, increased GSH level by 59.5, 64.6, and 65.1%, and reduced LPO level by 89.4, 90.0 and 90.5%, respectively (Table 3).

Nociceptive responses assessment

Thermal and tactile neurological-functions were evaluated every other week for 8 weeks post-treatment exploiting hot-plate latency (HPL), tail-flick latency (TFL), and von Frey filament paw-withdrawal thresholds (PWT) methods (Figures 8, 9 and 10).

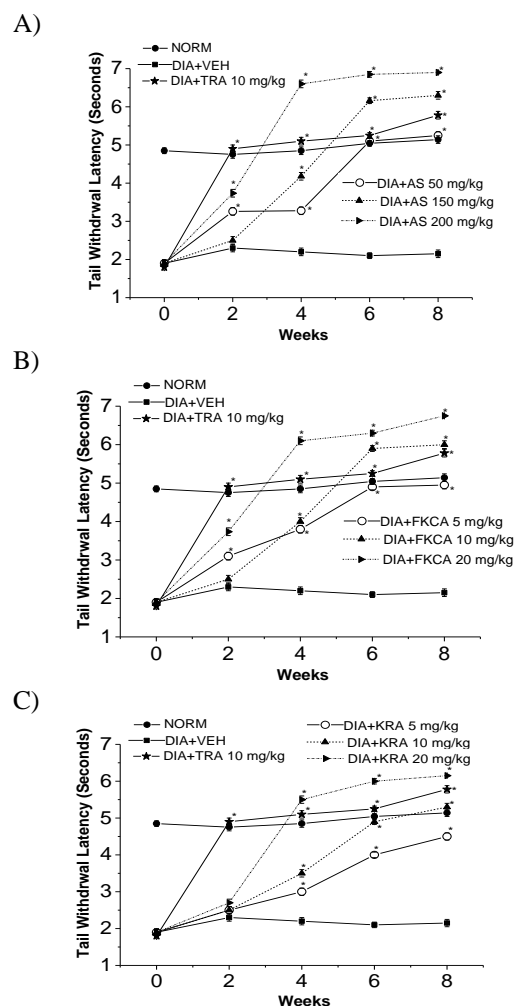


Figure 9. The effect of (A) *Acanthus syriacus* (AC), (B) FKCA isolated fraction (FKCA), and (C) kromelic acid (KRA) against hyperalgesia in terms of tail-flick latency in alloxan-treated mice treated with tramadol (TRA 10mg/kg) as a positive control. "NORM" designates normal non-diabetic mice. "*" shows significant differences at $p < 0.05$ compared to vehicle diabetic-control (DIA+VEH), (n=7).

Thermal-pain responses

After 8 weeks of oral administration of different treatments, as compared to VEH, the orally-administrated AS 50, 100 and 150mg/kg provoked a significant rise in the thermal-stimuli reaction-time by 0.88, 1.07 and 1.00 folds for HPL, and by 1.44, 1.93 and 2.21 folds for TFL, respectively (Figures 8A and 9A). Also, FKCA administration at doses of 5, 10 and 20mg/kg, raised HPL by 0.96, 1.01 and 1.07 folds, and elevated TFL by 1.30, 1.79, and 2.16 folds, respectively (Figures 8B and 9B). Moreover, KRA oral administration at doses of 5, 10 and 20mg/kg raised HPL by 0.53, 0.65, and 0.80 folds, and raised TFL by 1.10, 1.47 and 1.86 folds, respectively (Figures 8C and 9C). These outcomes were evaluated against tramadol 10mg/kg (TRA), a positive control, which increased HPL by

0.94 folds, and TFL by 1.69 folds (Figures 8 and 9).

The efficiency of AS, FKCA, and KRA on amelioration of thermal hyperalgesia, proposes their antinociceptive properties against hyperalgesic-pain.

Tactile-nociceptive responses

The tactile allodynia was evaluated by assessing PWT exploiting Von-Frey filaments after 8-week oral administration of different treatments and compared to VEH group (Figure 10). AS at doses of 50, 100 and 150mg/kg induced a significant rise in PWT by 6.25, 6.40 and 6.77 folds, respectively (Figure 10). FKCA at doses of 5, 10 and 20mg/kg elevated PWT by 7.51, 8.06, and 8.25 folds, respectively (Figure 10). Also, KRA 5, 10 and 20 mg/kg raised PWT by 2.14, 2.33 and 2.88 folds, respectively (Figure 10). TRA elevated PWT by 8.87 folds (Figure 10).

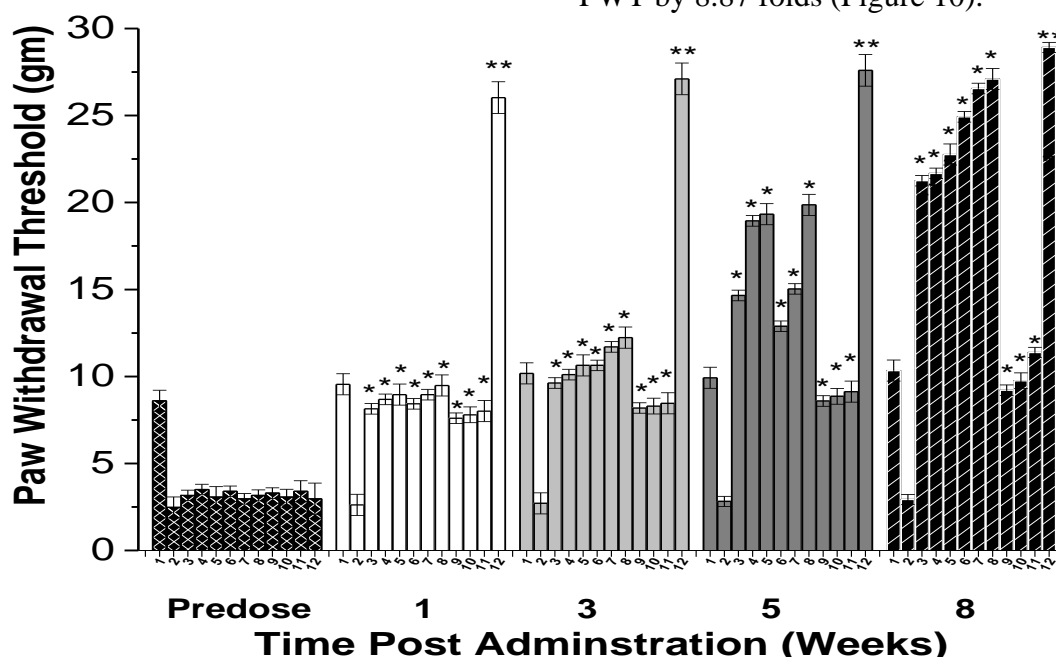


Figure 10. The effect of *Acanthus syriacus* (AC), FKCA isolated fraction (FKCA), kromeic acid (KRA), and tramadol (TRA) 10 mg/kg, on tactile allodynia in a neuropathic model; 1: (NORM) normal non-diabetic untreated mice, 2: VEH, 3: AS 50 mg/kg, 4: AS 100 mg/kg, 5: AS 150 mg/kg, 6: FKCA 5 mg/kg, 7: FKCA 10 mg/kg, 8: FKCA 20 mg/kg, 9: KRA 5 mg/kg, 10: KRA 10 mg/kg, 11: KRA 20 mg/kg, 12: TRA 10 mg/kg (n=7 animals/group). * $p < 0.05$ and ** $p < 0.01$ show significant differences compared to vehicle-treated animals (VEH).

AS, FKCA and KRA potentials against urinary and tissue nitrite level

One of the possible anti-neuropathic pain mechanisms of action of a given

compound is mediated through its potential to reduce nitrite level (Taliyan and Sharma, 2012). Thus, nitrite levels in the urine and heart left ventricle tissues were monitored

Acanthus syriacus phytochemical and biological investigation

pre- (control group) and 8-weeks post-treatment (test group), in order to explore the test compounds' antinociceptive mechanism. The vehicle-treated neuropathic animals significantly raised urinary and tissue nitrite concentration compared to normal control (Table 4). Compared to vehicle control, the AS (50, 100, and 150mg/kg) reduced urinary nitrite level (UNL) by 23.6, 53.3, 58.1%, respectively, and decreased tissue nitrite level (TNL) by 14.5, 48.9, 58.8%, 8-week post-treatment (Table 4). Eight-week oral

administration of FKCA (5, 10, and 20mg/kg) declined UNL by 22.0, 50.8, 59.3%, respectively, and reduced TNL by 20.8, 40.3, and 60.6%, whereas KRA (5, 10, 20mg/kg) declined UNL by 17.4, 38.7, and 48.6%, respectively, and decreased TNL by 16.9, 32.3, and 46.6%, respectively, compared to vehicle control (Table 4). The positive control, MTF, had no significant effect on UTL or TNL (Table 4).

Table 3. *In-vivo* assessment of the antioxidant activities of *Acanthus syriacus* (AC), FKCA isolated fraction (FKCA), and kromeic acid (KRA) on serum levels of CAT, reduced GSH, and alterations in TBARS (n=7/group; data presented as Mean \pm SEM).

Group	Dose (mg/kg)	Catalase level (kU/l)		GSH (μ g/mg)		TBARS Level (nM/100g)	
		Predose	8 weeks	Predose	8 weeks	Predose	8 weeks
Normal control	—	32.03 \pm 1.40	31.05 \pm 1.58	60.30 \pm 1.09	60.70 \pm 1.08	0.87 \pm 0.01	0.84 \pm 0.01
Vehicle control	—	22.16 \pm 1.00	16.70 \pm 1.13	55.53 \pm 1.60	39.50 \pm 1.50	0.98 \pm 0.02	5.30 \pm 0.01
MTF ^a	25	21.93 \pm 1.13	22.98 \pm 1.18	55.10 \pm 1.40	53.90 \pm 1.30	1.02 \pm 0.01	1.35 \pm 0.02
AS ^a	50	22.54 \pm 1.03	38.87 \pm 1.25*	55.43 \pm 1.50	74.07 \pm 1.00*	0.91 \pm 0.01	0.41 \pm 0.01*
AS ^a	100	22.88 \pm 1.21	41.85 \pm 1.30*	54.56 \pm 1.40	74.52 \pm 1.10*	0.93 \pm 0.02	0.42 \pm 0.02*
AS ^a	150	22.74 \pm 2.25	42.97 \pm 1.37*	56.48 \pm 1.10	77.16 \pm 1.20*	0.90 \pm 0.02	0.39 \pm 0.04*
FKCA ^a	5	23.10 \pm 1.46	38.10 \pm 1.05*	56.39 \pm 1.40	73.01 \pm 1.50*	0.90 \pm 0.01	0.42 \pm 0.02*
FKCA ^a	10	22.10 \pm 1.05	40.95 \pm 1.60*	57.96 \pm 1.10	73.60 \pm 1.10*	0.94 \pm 0.02	0.44 \pm 0.02*
FKCA ^a	20	23.41 \pm 1.60	43.05 \pm 1.51*	57.44 \pm 1.20	78.30 \pm 1.20*	0.89 \pm 0.03	0.38 \pm 0.01*
KRA ^a	5	22.29 \pm 1.38	30.11 \pm 1.35*	56.04 \pm 1.10	63.02 \pm 1.10*	1.06 \pm 0.01	0.56 \pm 0.01*
KRA ^a	10	22.17 \pm 1.03	32.32 \pm 1.04*	57.18 \pm 1.30	65.00 \pm 1.00*	0.95 \pm 0.02	0.53 \pm 0.01*
KRA ^a	20	22.70 \pm 1.68	33.60 \pm 1.05*	55.61 \pm 1.60	65.20 \pm 1.40*	0.90 \pm 0.01	0.50 \pm 0.02*

SEM.: mean standard error

* p<0.05 indicates significant differences from the vehicle control animals.

^aCompared to vehicle control.

Table 4. Effect of interventions on urinary and tissue nitrite level.

Group	Dose (mg/kg)	Urinary nitrite level (μ M/L)		Tissue nitrite level (μ M/mg protein)	
		Predose	8 weeks	Predose	8 weeks
Normal control	—	16.04 \pm 0.90	16.20 \pm 1.40	3.68 \pm 0.94	3.90 \pm 0.96
Vehicle control	—	37.97 \pm 1.94	41.76 \pm 1.92	11.48 \pm 0.50	12.63 \pm 0.60
MTF ^a	25	36.65 \pm 1.01	34.65 \pm 2.10	10.10 \pm 1.22	9.02 \pm 1.00
AS ^a	50	35.80 \pm 0.94	31.89 \pm 1.00*	11.53 \pm 0.39	10.80 \pm 0.60*
AS ^a	100	35.88 \pm 0.98	19.50 \pm 1.10*	12.01 \pm 0.45	6.45 \pm 0.50*
AS ^a	150	36.01 \pm 1.09	17.47 \pm 1.07*	11.56 \pm 0.6	5.20 \pm 0.50*
FKCA ^a	5	35.78 \pm 1.16	32.56 \pm 0.95*	11.25 \pm 0.50	10.00 \pm 0.40*
FKCA ^a	10	36.02 \pm 0.94	20.55 \pm 1.30*	10.98 \pm 0.40	7.54 \pm 0.45*
FKCA ^a	20	37.10 \pm 1.30	16.98 \pm 1.21*	11.24 \pm 0.42	4.98 \pm 0.65*
KRA ^a	5	36.22 \pm 1.08	34.50 \pm 1.05*	11.35 \pm 0.43	10.50 \pm 0.42*
KRA ^a	10	36.55 \pm 1.05	25.60 \pm 1.03*	11.55 \pm 0.47	8.55 \pm 0.45*
KRA ^a	20	36.33 \pm 1.38	21.45 \pm 0.90*	11.89 \pm 0.39	6.75 \pm 0.44*

SEM.: mean standard error

* p<0.05 indicates significant differences from the vehicle control animals.

^aCompared to vehicle control.

Discussion

The phytochemical investigation, the bio-guided fractionation, and isolation schemes conducted in this study utilizing various chromatographic, NMR, and biological inflammatory and NP models, showed that *A. syriacus* most active fraction was the isolated FKCA fraction. Chromatographic methods identified ferulic and chlorogenic acids as two of the three components of FKCA by. The third compound was a quinic acid derivative elucidated by various analytical methods especially, ^1H and ^{13}C NMR method. The quinic acid derivative (compound 3) was named kromeic acid (KRA), and the most active fraction in *A. syriacus* (AS) was FKCA due to its content of Ferulic acid (27.5%), kromeic acid (48.1%), and chlorogenic acid (24.4%).

Moreover, the significant efficiency of the tested compounds with respect to raising SIL, implies that the insulin-secretagogue activity is amongst diabetes controlling mechanisms of AS, FKCA, and KRA. These results are similar to previous reports indicating *Prunus cerasus* and *Anemone coronaria* secretagogue potential as one of their anti-diabetic mechanisms of action (Raafat and El-Lakany, 2018; Saleh et al., 2017).

The antioxidant potentials of AS, FKCA, and KRA on elevating CAT and GSH, and reducing LPO levels, propose their potentials in ameliorating painful-neuropathy. Earlier studies on compounds with similar antioxidant potentials, also found antinociceptive properties (Muthuraman et al., 2008; Nishiyama and Ogawa, 2005).

AS, FKCA, and KRA ameliorating potentials on mechanical-nociceptive propose their antinociceptive activities against allodynic-pain. These results are aligned with earlier studies that suggested a neuroprotective effect for other natural-compounds, like Curcuma sesquiterpenes and *Ginkgo biloba* polyphenolics, against neurotoxicity (Hibatallah et al., 1999; Raafat and Omar, 2016; Shi et al., 2010).

Also, AS, FKCA, and KRA protective effects against NO-induced neuronal toxicity might be one of the test compounds' possible antinociceptive mechanisms as described before for *G. biloba* extract and other natural compounds (Green et al., 1982; Taliyan and Sharma, 2012).

AS, FCKA, and KRA showed significant anti-inflammatory activities. Compared to TRA, highest doses of AS, FKCA, and KRA showed higher antinociceptive potentials in controlling allodynic and thermal-hyperalgesic NP. AS and FCKA showed relatively equipotent antinociceptive effects with a predominant ameliorating effect of FCKA at its highest dose (20mg/kg). FKCA had more marked antinociceptive effects than KRA suggesting additive effects of FKCA components strengthening its anti-neuropathic potentials. The insulin-secretagogue, anti-inflammatory, anti-oxidative-stress, and protective effects against NO-induced neuronal toxicity potentials may be amongst AS, FKCA and KRA mechanisms through which they alleviated neuropathic-pain.

After conducting clinical-trials, *A. syriacus*, FKCA, and KRA might be used as a novel complementary approach for alleviation of a variety of painful-syndromes.

Acknowledgment

Many thanks for proof-reading the manuscript by Mrs. G. Onsy.

Conflicts of interest

No conflicts of interest to be declared.

References

- Asongalem EA, Foyet HS, Ekobo S, Dimo T, Kamtchouing P. 2004. Antiinflammatory, lack of central analgesia and antipyretic properties of *Acanthus montanus* (Ness) T. Anderson. *J Ethnopharmacol*, 95:63-68.
- Babu BH, Shylesh BS, Padikkala J. 2001. Antioxidant and hepatoprotective effect of

Acanthus syriacus phytochemical and biological investigation

- Acanthus ilicifolius*. *Fitoterapia*, 72:272-277.
- Babu BH, Shylesh BS, Padikkala J. 2002. Tumour reducing and anticarcinogenic activity of *Acanthus ilicifolius* in mice. *J Ethnopharmacol*, 79:27-33.
- Baydoun S, Chalak L, Dalleh H, Arnold N. 2015. Ethnopharmacological survey of medicinal plants used in traditional medicine by the communities of Mount Hermon, Lebanon. *J Ethnopharmacol* 173:139-156.
- Bravo HR, Copaja SV, Argandona VH. 2004. Chemical basis for the antifeedant activity of natural hydroxamic acids and related compounds. *J Agric Food Chem*, 52:2598-2601.
- Cameron NE, Cotter MA. 2008. Pro-inflammatory mechanisms in diabetic neuropathy: focus on the nuclear factor kappa B pathway. *Curr Drug Targets*, 9:60-67.
- Capanlar S, Boke N, Yasa I, Kirmizigul S, 2010. A novel glycoside from *Acanthus hirsutus* (Acanthaceae). *Nat Prod Commun*, 5:563-566.
- Comelli F, Bettoni I, Colleoni M, Giagnoni G, Costa B. 2009. Beneficial effects of a *Cannabis sativa* extract treatment on diabetes-induced neuropathy and oxidative stress. *Phytother Res*, 23:1678-1684.
- Ellman GL. 1959. Tissue sulfhydryl groups. *Arch Biochem Biophys*, 82:70-77.
- Gardmark M, Hoglund AU, Hammarlund-Udenaes M. 1998. Aspects on tail-flick, hot-plate and electrical stimulation tests for morphine antinociception, *Pharmacol Toxicol*. 83:252-258.
- Green LC, Wagner DA, Glogowski J, Skipper PL, Wishnok JS, Tannenbaum SR. 1982. Analysis of nitrate, nitrite, and [15N] nitrate in biological fluids. *Anal Biochem*.126:131-138.
- HibatallahJ, Carduner C, Poelman MC. 1999. In-vivo and in-vitro assessment of the free-radical-scavenger activity of Ginkgo flavone glycosides at high concentration. *J Pharm Pharmacol*, 51:1435-1440.
- Jamalan M, Rezazadeh M, Zeinali M, Ghaffari MA. 2015. Effect of ascorbic acid and alpha-tocopherol supplementations on serum leptin, tumor necrosis factor alpha, and serum amyloid A levels in individuals with type 2 diabetes mellitus. *Avicenna J Phytomed*, 5:531-539.
- Joharchi K, Jorjani M. 2007. The role of nitric oxide in diabetes-induced changes of morphine tolerance in rats. *Eur J Pharmacol*, 570:66-71.
- Khaneshi F, Nasrolahi O, Azizi S, Nejati V. 2013. Sesame effects on testicular damage in streptozotocin-induced diabetes rats. *Avicenna J Phytomed*, 3:347-355.
- Micov A, Tomić M, Pecikoza U, Ugrešić N, Stepanović-Petrović R. 2015. Levetiracetam synergises with common analgesics in producing antinociception in a mouse model of painful diabetic neuropathy. *Pharmacol Res*. 97:131-142.
- Muthuraman A, Diwan V, Jaggi AS, Singh N, Singh D. 2008. Ameliorative effects of *Ocimum sanctum* in sciatic nerve transection-induced neuropathy in rats. *J Ethnopharmacol*, 120:56-62.
- Nishiyama T, Ogawa M. 2005. Intrathecal edaravone, a free radical scavenger, is effective on inflammatory-induced pain in rats. *Acta Anaesthesiol Scand*, 49:147-151.
- Ohkawa H, Ohishi N, Yagi K. 1979. Assay for lipid peroxides in animal tissues by thiobarbituric acid reaction. *Anal Biochem*, 95:351-358.
- Ohsawa M, Aasato M, Hayashi SS, Kamei J. 2011. RhoA/Rho kinase pathway contributes to the pathogenesis of thermal hyperalgesia in diabetic mice. *Pain*, 152:114-122.
- Ozkul A, Ayhan M, Yenisey C, Akyol A, Guney E, Ergin FA. 2010. The role of oxidative stress and endothelial injury in diabetic neuropathy and neuropathic pain. *Neuro Endocrinol Lett*, 31:261-264.
- Pabbidi RM, Cao DS, Parihar A, Pauza ME, Premkumar LS. 2008. Direct role of streptozotocin in inducing thermal hyperalgesia by enhanced expression of transient receptor potential vanilloid 1 in sensory neurons. *Mol Pharmacol*, 73:995-1004.
- Raafat K, El-Darra N, Saleh FA, Rajha HN, Maroun RG, Louka N. 2017a. Infrared-assisted extraction and HPLC-analysis of *Prunus armeniaca* L. pomace and detoxified-kernel and their antidiabetic effects. *Phytochem Anal*, 1:1-12.
- Raafat K, El-Haj R, Shoumar D, Alaaeddine R, Fakhro Y, Tawil N, Shaer F, Daher A, Awada N, Sabra A, Atwi K, Khaled M, Messi R, Abouzaher N, Houry M, Al Jallad S. 2017b. Neuropathic pain: literature

- review and recommendations of potential phytotherapies. *Pharmacog J* 9:1-10.
- Raafat K, El-Lakany A. 2018. Phytochemical and antinociceptive investigations of anemone coronaria active part ameliorating diabetic neuropathic pain. *Planta Med Int Open*, 5: e5-e13.
- Raafat K, Hdaib F. 2017. Neuroprotective effects of *Moringa oleifera*: bio-guided GC-MS identification of active compounds in diabetic neuropathic pain model. *Chin J Integr Med*. 1:e1-e10.
- Raafat K, Wael S. 2018. Phytochemical and biological evaluation of ultrasound-assisted spray dried *Lonicera etrusca* for potential management of diabetes records of natural products, 12:367-379.
- Raafat KM, Omar AG. 2016. Phytotherapeutic activity of curcumin: Isolation, GC-MS identification, and assessing potentials against acute and subchronic hyperglycemia, tactile allodynia, and hyperalgesia. *Pharm Biol*, 54:1334-1344.
- Salama RAM, El Gayar NH, Georgy SS, Hamza M. 2016. Equivalent intraperitoneal doses of ibuprofen supplemented in drinking water or in diet: a behavioral and biochemical assay using antinociceptive and thromboxane inhibitory dose-response curves in mice. *Peer J*, 4: e2239.
- Saleh FA, El-Darra N, Raafat K. 2017. Hypoglycemic effects of *Prunus cerasus* L. pulp and seed extracts on alloxan-induced diabetic mice with histopathological evaluation. *Biomed Pharmacother*, 88:870-877.
- Shi C, Liu J, Wu F, Yew DT. 2010. Ginkgo biloba extract in Alzheimer's disease: from action mechanisms to medical practice. *Int J Mol Sci*, 11:107-123.
- Sullivan KA, Hayes JM, Wiggin TD, Backus C, Su Oh S, Lentz SI, Brosius F. 3rd, Feldman, EL. 2007. Mouse models of diabetic neuropathy. *Neurobiol Dis*, 28:276-285.
- Taliyan R, Sharma PL. 2012. Protective effect and potential mechanism of Ginkgo biloba extract EGb 761 on STZ-induced neuropathic pain in rats. *Phytother Res*, 26:1823-1829.
- Willoughby DA, DiRosa M. 1972. Studies on the mode of action of non-steroid anti-inflammatory drugs. *Ann Rheum Dis*, 31: 540-551.
- Yasmineh WG, Kaur TP, Blazar BR, Theologides A. 1995. Serum catalase as marker of graft-vs-host disease in allogeneic bone marrow transplant recipients: pilot study. *Clin Chem*, 41: 1574-1580.
- Ziegler D. 2008. Treatment of diabetic neuropathy and neuropathic pain: how far have we come? *Diabetes Care*. 31 Suppl 2: S255-261.
- Ziegler D. 2010. [Can diabetic polyneuropathy be successfully treated?]. *MMW Fortschr Med*, 152:64-68.